

H_{c2} MEASUREMENTS OF Nb_3Sn AND NITROGEN-DOPED NIOBIUM USING PHYSICAL PROPERTY MEASUREMENT SYSTEM*†

J. T. Maniscalco‡, D. Gonnella, D. L. Hall, M. Liepe, and S. Posen
 CLASSE, Cornell University, Ithaca, NY, 14853, USA

Abstract

The measurement of the upper critical field of a type-II superconductor, H_{c2} , is an important step in determining its superconducting properties, and therefore its suitability as a material in SRF cavities. However, measuring H_{c2} directly can be challenging, as performing electrical measurements causes changes in the very properties one seeks to measure. We present a method for extracting H_{c2} from resistivity measurements made near the transition temperature for varied applied fields and excitation currents. We also present first results of these measurements made on Nb_3Sn and nitrogen-doped niobium.

INTRODUCTION

In the field of superconducting radio frequency (SRF) accelerators, niobium has had a long and successful career as the fabrication material of choice. However, as accelerator demands increase, the field is behooved to find new materials with improved qualities. One promising type of new material is surface-treated niobium, *i.e.* bulk niobium with a thin layer of a different material on the RF-active surface. In this paper we investigate the properties of two such materials, namely Nb_3Sn and nitrogen-doped niobium; we develop a method for finding the upper critical field of a material, from which one can calculate many other figures of merit, including the coherence length ξ and the mean free path ℓ .

The upper critical field H_{c2} of a type-II superconductor is the minimum magnetic field at which the material cannot superconduct, regardless of temperature. This field is very difficult to observe directly, as it requires holding the temperature of the sample at absolute zero while measurements are made. Instead, it must be extrapolated from measurements of the superconducting transition at higher temperatures.

The Physical Property Measurement System (PPMS, Quantum Design) and machines like it allow the researcher to perform low-temperature electrical and magnetic measurements with direct control over the temperature and applied magnetic field at the sample. Using such a machine, we can set a magnetic field and measure the resistivity of a sample of the material of interest, for a chosen magnetic field and temperature, with a lower bound of 1.9 K for the temperature and an upper bound of 9 T for the field.

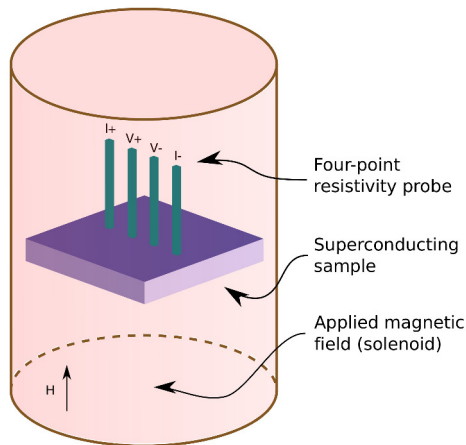


Figure 1: Schematic of testing environment inside PPMS. Spring-loaded press contacts act as a four-point resistivity probe on the surface of the superconducting material. The apparatus sits inside a solenoid, which applies an external magnetic field.

METHOD

At a given applied magnetic field strength, a superconductor will transition to its normal-conducting state at some temperature T . We can invert this function to get $H_{c2}(T)$, the magnetic field where, for a given temperature, the material makes its phase transition. Given a set of measurements of transitions with values of T and $H_{c2}(T)$, we can extrapolate the upper critical field $H_{c2} = H_{c2}(0)$ and the critical temperature T_c using Eq. 1 [1]¹:

$$H_{c2}(0) = H_{c2}(T) \left[1 - \left(\frac{T}{T_c(0)} \right)^2 \right]^{-1} \quad (1)$$

In order to perform these measurements, we use the PPMS to perform four-point resistivity measurements on the sample at fixed magnetic fields and varying temperature. For these measurements, four needles are pressed against the surface of the sample and a 17 Hz AC signal is applied between the first and fourth pins for a short time. While the current is being applied, the voltage across the two center pins is measured, and the PPMS calculates and records the resistivity. Figure 1 shows the typical experimental setup. In the superconducting

¹ This dependence is approximate, see for example [2]

* Funding provided by NSF grants PHY-1305500 and PHY-1416318.

† This work made use of the Cornell Center for Materials Research Shared Facilities which are supported through the NSF MRSEC program (DMR-1120296).

‡ jtm288@cornell.edu

state, the resistivity is zero; in the normal-conducting state, the resistivity is finite.

Figures 2 and 3 show two examples of the resulting output from the PPMS, with resistivity at varying temperatures. Since the transition to the superconducting state is not instantaneous throughout the sample, there is a gradient in the resistivity across the transition. We take the average temperature of the transition region as the critical temperature, and take half the width of the region as the uncertainty.

The resistivity measurement process introduces another complication: current passing through the superconductor also affects the transition, with higher current corresponding to a lower transition temperature. To account for this, we perform the resistivity vs. temperature measurements for a fixed field at several different excitation currents, then extrapolate the T_c vs. I points linearly to zero excitation current according to Eq. 2 (where m is some proportionality constant):

$$T_c(I = 0, H) = T_c(I, H) - I \times m \quad (2)$$

We chose a linear fit because it most closely fits the data at all fields. After performing this extrapolation on the resistivity data, we are left with a set of T_c vs H points from which we can extrapolate H_{c2} using Eq. 1.

Once we have determined H_{c2} for a given sample, we can calculate other figures of interest to SRF applications. The Ginzburg Landau coherence length ξ and upper critical field are related by Eq. 3 [2], where Φ_0 is the flux quantum:

$$H_{c2} = \frac{\Phi_0}{2\pi\xi^2} \quad (3)$$

From there we can determine the mean free path ℓ given the “clean coherence length” ξ_0 for the bulk material (for treated niobium we can use the coherence length of plain niobium, $\xi_0 = 38$ nm) [3] with Eq. 4 [4]:

$$\xi = 0.739 \left[\xi_0^{-2} + \frac{0.882}{\xi_0 \ell} \right]^{-1/2} \quad (4)$$

Further, we can use the London penetration depth of clean niobium $\lambda_L = 39$ nm [3] to find the Ginzburg Landau parameter κ for the “dirty” material using Eq. 5 [5]:

$$\kappa = \frac{\lambda_L}{\xi} \sqrt{1 + \frac{\xi_0}{\ell}} \quad (5)$$

RESULTS

Figures 2 and 3 show typical resistivity vs. temperature curves for given fixed fields and excitation currents. An interesting feature visible in some of the resistivity-temperature curves for the N-doped samples, as seen in Fig. 2, is a “double hump”, what appears to be a splitting of the superconducting transition into two separate parts. We believe

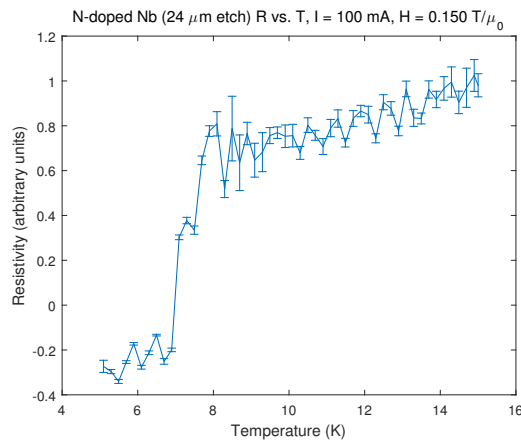


Figure 2: Resistivity vs. temperature for a nitrogen-doped niobium sample, with a 24 μm etch, measured with excitation current $I = 100$ mA and applied field $H = 150$ mT/ μ_0 . Note that the flat superconducting region at left shows resistivity below zero; this is a systematic error due to a phase difference introduced in the AC measurements. Error bars show statistical uncertainty.

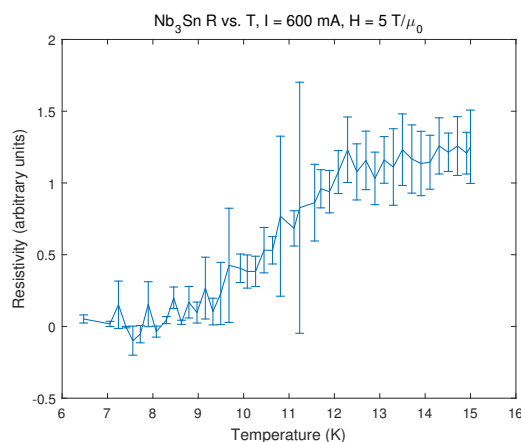


Figure 3: Resistivity vs. temperature for a Nb_3Sn sample, measured with excitation current $I = 600$ mA and applied field $H = 5$ T/ μ_0 .

that the upper transition corresponds with the surface material, while the lower transition corresponds with the bulk material. For the purposes of finding H_{c2} , we have used the transition temperatures of the upper transitions.

Figures 4, 5, and 6 show the compiled transition temperature data on the temperature-field plane for Nb_3Sn , 24 μm -etched N-doped Nb, and 48 μm -etched N-doped Nb, respectively. Table 1 compiles the calculations of H_{c2} and T_c for the three samples. Table 2 shows the results of the calculations of the coherence length ξ , mean free path ℓ , and Ginzburg Landau parameter κ , according to Eqs. 3-5.

To determine the uncertainty in H_{c2} , we placed a lower bound on the uncertainty interval by taking the highest field at which we could observe a superconducting transition. For our calculations, we took the fitted value as the center of the interval, with the upper bound equally spaced on the upper

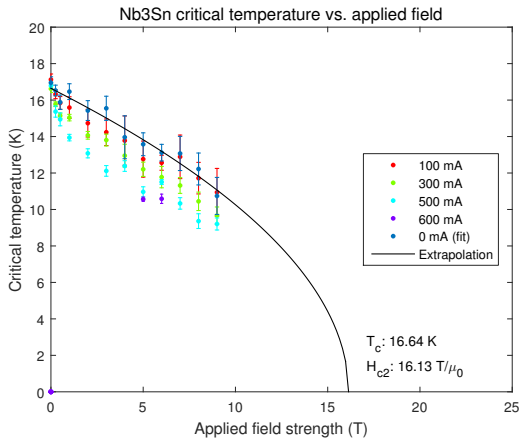


Figure 4: Superconducting transition data for Nb₃Sn, with H_{c2} extrapolation. For this sample we found $T_c = 16.64$ K and $H_{c2} = 16.13$ T/ μ_0 .

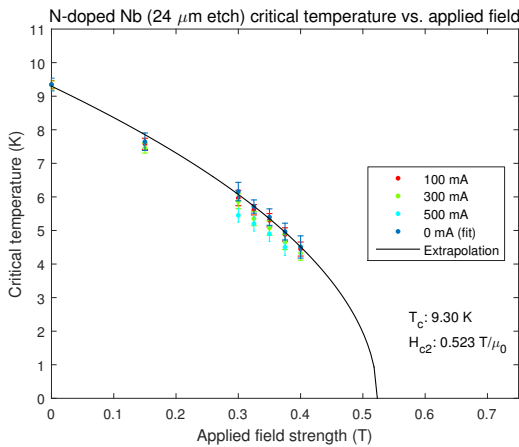


Figure 5: Superconducting transition data for N-doped niobium, 24 μm etch, with H_{c2} extrapolation. For this sample we found $T_c = 9.19$ K and $H_{c2} = 0.456$ T/ μ_0 .

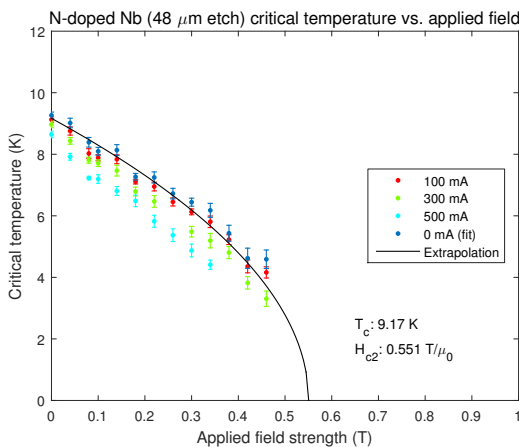


Figure 6: Superconducting transition data for N-doped niobium, 48 μm etch, with H_{c2} extrapolation. For this sample we found $T_c = 9.28$ K and $H_{c2} = 0.501$ T/ μ_0 .

Table 1: Upper Critical Field and Critical Temperature

Material	H_{c2} (T)	T_c (K)
Nb ₃ Sn	16.13	16.64
N-doped Nb (24 μm etch)	0.52 ± 0.12	9.30
N-doped Nb (48 μm etch)	0.55 ± 0.11	9.17

Table 2: Coherence Length, Mean Free Path, and Ginzburg Landau Parameter

Material	ξ (nm)	ℓ (nm)	κ
Nb ₃ Sn	4.517	19.82	22.92
N-doped Nb (24 μm etch)	25.1 ± 2.9	$130(-80, +5000)^1$	1.8 ± 0.4
N-doped Nb (48 μm etch)	24.4 ± 2.5	$100(-50, +270)^1$	1.9 ± 0.4

¹ Uncertainty range is wide due to the fact that Eq. 4 gives an infinite value for the mean free path ℓ as the coherence length ξ approaches $0.739 \times \xi_0$; for niobium, this limit is $\xi \rightarrow 28.08$.

side of the interval. However, we did not use this technique for the Nb₃Sn sample, since for those measurements we were limited by the maximum magnetic field of the PPMS to fields well below $H_{c2}(0)$.

Our calculation of $H_{c2}(0)$ for Nb₃Sn is in agreement with the literature [1]. However, our results for the nitrogen-doped Nb samples are significantly lower than what we would expect based on the material properties as extracted from RF measurements. It is possible that our measurements here are affected by the bulk material, which would lower the value of $H_{c2}(0)$. More work is needed to better understand this effect.

CONCLUSION & OUTLOOK

Directly measuring the upper critical field $H_{c2}(0)$ with electrical measurements is very difficult, due to the physical limitations of working near absolute zero. Electrical measurements are further complicated by the influence of electric current on the superconducting transition temperature. Using the method outlined above, however, it is possible to determine $H_{c2}(0)$ indirectly by first measuring the transition temperatures at varying currents and fields, then extrapolating along the phase transition surface to zero excitation current and zero temperature. With H_{c2} in hand, we can calculate other figures relevant to SRF studies, such as the coherence length ξ , mean free path ℓ , and Ginzburg Landau parameter κ .

Overall, these results are a good preliminary look at the properties of these materials. Looking forward, it will be very interesting to further investigate the double transition seen in the N-doped niobium samples. Understanding that behavior better will likely offer improvements to the extraction of $H_{c2}(0)$ for these materials and others like them.

REFERENCES

- [1] Samuel Elliot Posen. *Understanding and Overcoming Limitation Mechanisms in Nb₃Sn Superconducting RF Cavities*. PhD thesis, Cornell University, 2015.
- [2] Michael Tinkham. *Introduction to Superconductivity*. Dover Publications, Inc., 2 edition, 1996.
- [3] Charles Kittel. *Introduction to Solid State Physics*. John Wiley & Sons, Inc., 2005.
- [4] T. P. Orlando, E. J. McNiff, S. Foner, and M. R. Beasley. Critical fields, Pauli paramagnetic limiting, and material parameters of Nb₃Sn and V₃Si. *Phys. Rev. B*, 19:4545–4561, May 1979.
- [5] M. Hein. *High-Temperature-Superconductor Thin Films at Microwave Frequencies*. Springer, 1999.